



Dalton
Transactions

Recent advances in metal-mediated nitrogen oxyanion reduction using reductively borylated and silylated N-heterocycles

Journal:	<i>Dalton Transactions</i>
Manuscript ID	DT-FRO-11-2021-003740.R1
Article Type:	Frontier
Date Submitted by the Author:	19-Dec-2021
Complete List of Authors:	Beagan, Daniel M.; Indiana University Cabelof, Alyssa; Indiana University Bloomington, Department of Chemistry

SCHOLARONE™
Manuscripts

Recent advances in metal-mediated nitrogen oxyanion reduction using reductively borylated and silylated N-heterocycles

Daniel M. Beagan and Alyssa C. Cabelof

Abstract

The reduction of nitrogen oxyanions is critical for the remediation of eutrophication caused by anthropogenic perturbations to the natural nitrogen cycle. There are many approaches to nitrogen oxyanion reduction, and here we report our advances in reductive deoxygenation using pre-reduced N-heterocycles. We show examples of nitrogen oxyanion reduction using Cr, Fe, Co, Ni, and Zn, and we evaluate the role of metal choice, number of coordinated oxyanions, and ancillary ligands on the reductive transformations. We report the experimental challenges faced and provide an outlook on new directions to repurpose nitrogen oxyanions into value-added products.

Introduction

The introduction of the industrial Haber-Bosch process¹ revolutionized the large-scale production of ammonia necessary to feed and sustain a growing population, but also brought many unforeseen environmental consequences.² Much of the ammonia that is introduced as fertilizer is converted to nitrate by organisms in the soil, and the high solubility of nitrate leads to accumulation of this environmental pollutant in many aquatic ecosystems.³ The increased concentration of high oxidation state nitrogen oxyanions results in eutrophication, leading to hypoxic environments and dead zones.⁴ Furthermore, many of these eutrophic ecosystems provide drinking water to local citizens, posing a direct threat to human health and creating a broader socioeconomic impact.⁵⁻⁷ An approach to mitigate anthropogenic perturbation to the natural nitrogen cycle is *via* reduction of high oxidation state nitrogen oxyanion pollutants, which is a challenge that has garnered attention in several areas of chemistry, including by materials chemists,⁸⁻¹⁴ photochemists,¹⁵⁻¹⁸ and electrochemists.¹⁹⁻²³ A common thread across different areas of chemistry in the reduction of nitrate is removal of an oxygen atom, which results in reduction of the nitrogen atom. To accomplish deoxygenation, an electrophile is required to sequester the removed oxygen. Examples in the literature of electrophiles for nitrate deoxygenation include low valent metals,²⁴⁻²⁷ carbon monoxide,²⁸ and protons.^{29, 30} The use of protons for nitrate reduction is coupled with electron transfer, often in an aqueous solution. Heterogenous systems that facilitate nitrogen oxyanion reduction boast efficiency, but often at the expense of mechanistic understanding and selectivity. Several recent examples of homogenous nitrate reduction have come from the Gilbertson,³¹ Lee,²⁸ and Fout³² groups (Figure 1c).

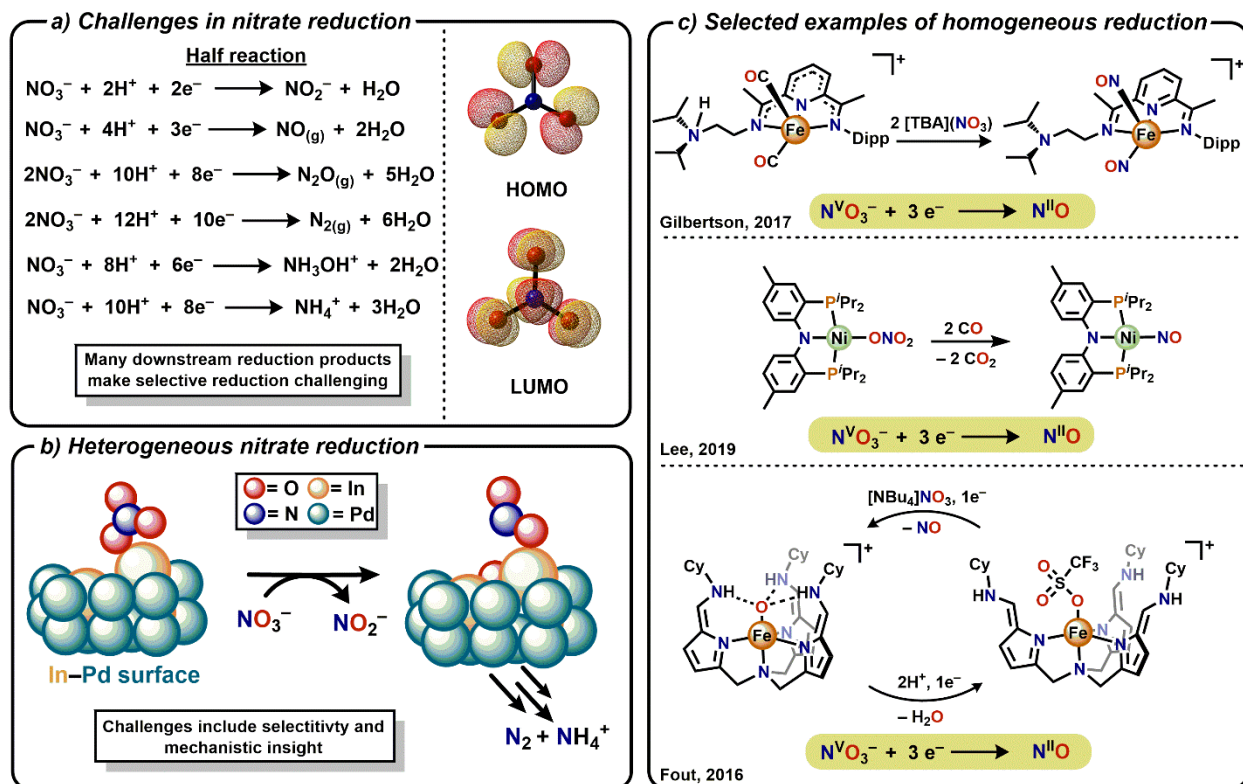
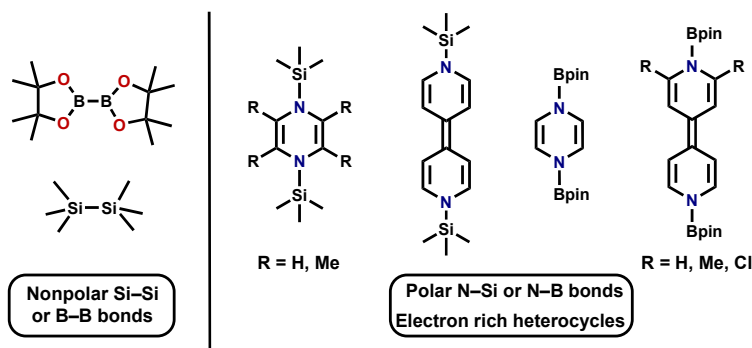


Figure 1. a) Half reactions showing the array of products that can be formed from nitrate reduction and the HOMO and LUMO of nitrate, b) selected example of heterogeneous nitrate reduction, and c) recent examples of homogeneous nitrate reduction from the Gilbertson (top), Lee (middle) and Fout (bottom) groups.

We target homogenous nitrogen oxanion reduction using pre-reduced N-heterocycles, which carry two electrons and two electrophiles necessary for reduction of the nitrogen atom and removal of O^{2-} . For homogenous reduction, one experimental challenge is coordination of nitrate. Nitrate has poor σ -basicity due to charge delocalization in the HOMO and is not π -acidic despite the LUMO having π^* character (Figure 1a). Further, the number of protons (electrophiles) and electrons delivered can greatly influence product selectivity (Figure 1a). Therefore, we hypothesize that using reductants which deliver two electrons and two electrophiles can impart selective metal-mediated nitrogen oxanion reduction. The N-heterocycles employed in our lab are silyl or boryl substituted pyrazines and 4,4'-bipyridines (Scheme 1).



Scheme 1. Silyl and boryl reduced heterocycles available for deoxygenation reactions and their nonpolar counterparts.

Silyl substituted reduced N-heterocycles were first synthesized by Kaim,^{33, 34} and later pioneered by Mashima,³⁵ and are used for salt free reduction of transition metal complexes,³⁶⁻³⁸ cyclopropanations,³⁹ and a variety of metal free deoxygenations of organic substrates.⁴⁰ Likewise, pioneered by Suginome,⁴¹ the boryl substituted reduced N-heterocycles are employed in organocatalytic deoxygenations,⁴² reductions of alkynes,⁴³ and de-aromatization of substituted pyrazines (Figure 2).⁴⁴

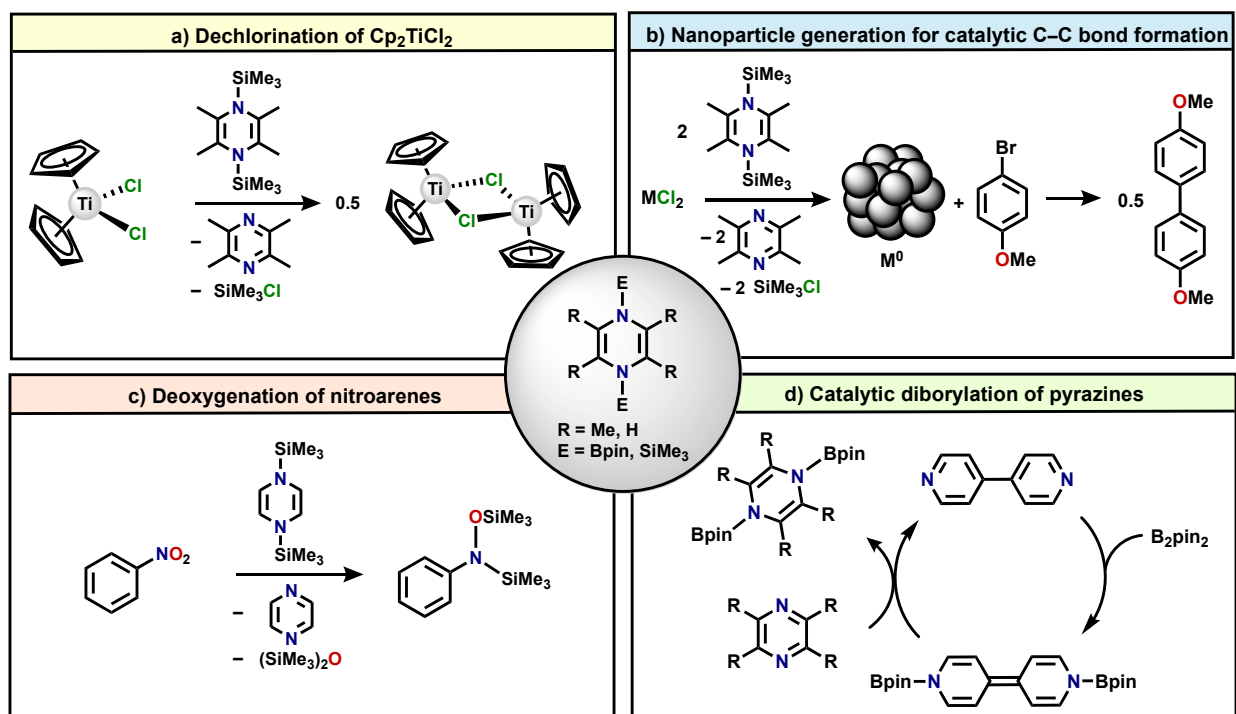
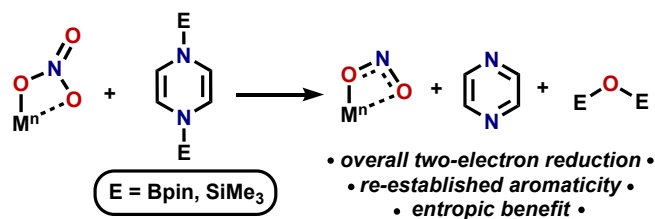


Figure 2. Examples from the Mashima (a-c) and Suginome (d) groups utilizing silyl or boryl substituted reduced N-heterocycles.

In our group, we have expanded the organic substrate scope of both the silylated and borylated N-heterocycles.^{45, 46} Importantly, we showed borylation of azobenzene and benzo-c-cinnoline, while the corresponding silylation does not occur.⁴⁶ We hypothesize that there is a mechanistic benefit to the empty boron p-orbitals in the reduced heterocycles which can accept electron density from a substrate Lewis-base.

The silyl and boryl substituted N-heterocycles are potent oxygen atom abstracting agents for several reasons. The resulting E–O (E = B, Si) bonds formed are strong due to the high oxophilicity of these heteroatoms, and re-aromatization of the N-heterocycle provides a secondary thermodynamic benefit (Scheme 2). There is an entropic benefit to the formation of boryl or silyl ether, and the polarized E–N bonds in the starting reagents provide a kinetic benefit for bond cleavage over an unpolarized bond in B₂pin₂ or (SiMe₃)₂ (Scheme 1).



Scheme 2. General scheme for deoxygenation of a metal nitrate complex to give a metal nitrite, representing a two electron reduction of the nitrogen atom in the oxyanion.

For these reasons, we have explored a variety of deoxygenations of coordinated N-oxyanion transition metal complexes using reduced N-heterocycles. Our goal is to study the influence of metal choice and number of coordinated oxyanions on the selectivity of the reduced nitrogen containing byproducts.

Results and Discussion

Deoxygenation of nitrate on chromium. In the interest of probing the selectivity of deoxygenation with multiple nitrate ligands coordinated to a single metal center, we synthesized the tris-nitrate complex, $(\text{H}_2\text{L})\text{Cr}(\text{NO}_3)_3$ (H_2L = bis(pyrazol-3-yl)pyridine). The $(\text{H}_2\text{L})\text{Cr}(\text{NO}_3)_3$ complex reacts with $(\text{SiMe}_3)_2\text{Pz}$ in a 1:2 mole ratio within 5 minutes, to form the nitrosyl complex, $(\text{H}_2\text{L})\text{Cr}(\text{NO}_3)_2(\text{NO})$ in 84% yield.⁴⁷ The paramagnetic nitrosyl complex is designated as a {CrNO} configuration, and an $S = \frac{1}{2}$ ground state is corroborated by EPR spectroscopy and a corresponding orbital analysis, which each indicate a chromium based SOMO (Figure 3b).

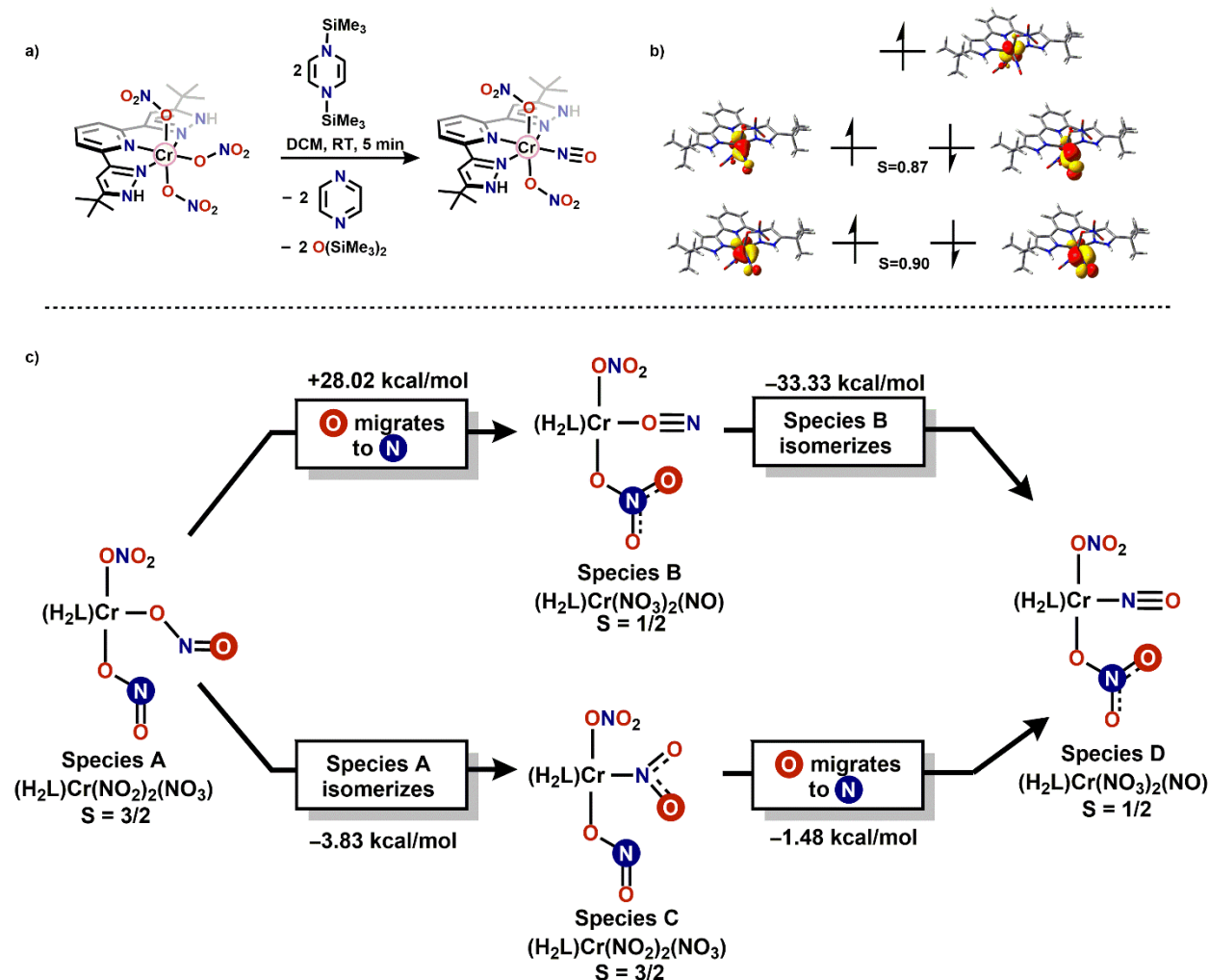
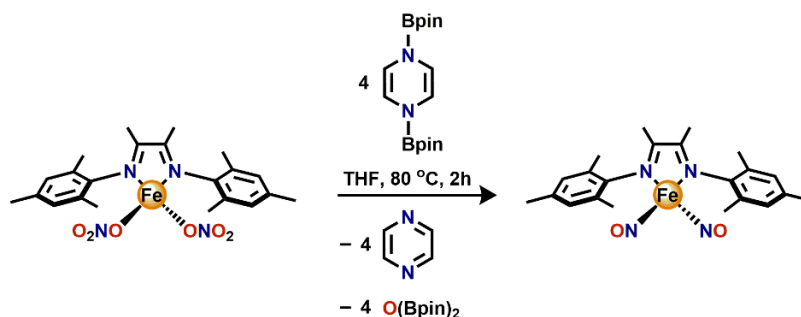


Figure 3. a) Synthesis of $(H_2L)Cr(NO_3)_2(NO)$ using $(SiMe_3)_2Pz$, b) corresponding orbital diagram for $(H_2L)Cr(NO_3)_2(NO)$, and c) DFT free energies of two isomerization mechanisms.

Density functional theory (DFT) calculations establish a viable pathway for this conversion to be deoxygenation of two different nitrate ligands, followed by isomerization of a nitrite and intramolecular oxygen atom transfer to reform a nitrate and a nitrosyl ligand (Figure 3c). This mechanistic pathway avoids the formation of a high energy isonitrosyl intermediate. Thermodynamic calculations for the overall transformation find the reaction to be highly exothermic (-158.1 kcal/mol), highlighting the thermodynamic potency of $(SiMe_3)_2Pz$ towards coordinated N-oxyanions.

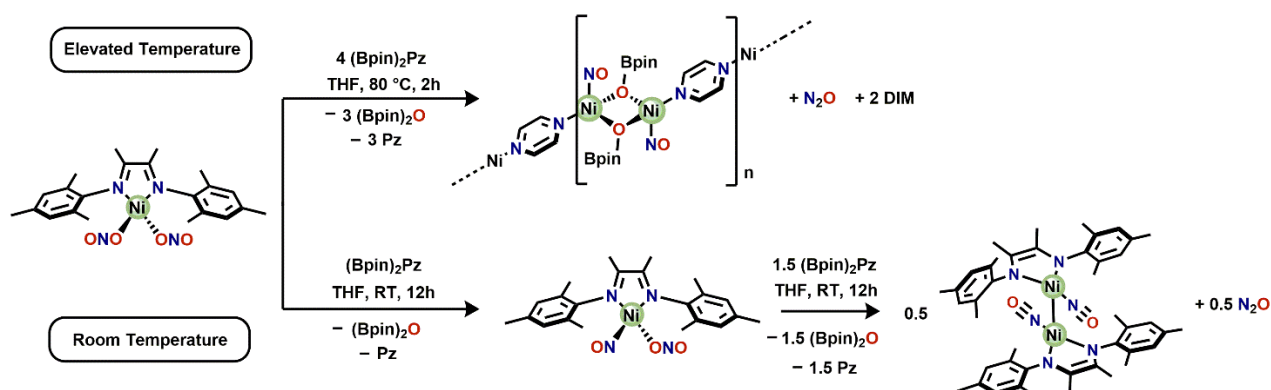
Deoxygenation of nitrate on iron. In an effort to decrease the number of coordinated nitrates, we synthesized $(DIM)Fe(NO_3)_2$ ($DIM = N,N'$ -bis(2,4,6-trimethylphenyl)-1,4-diaza-2,3-dimethyl-1,3-butadiene), which coordinates an acetonitrile molecule in the solid state. The reaction of $(DIM)Fe(NO_3)_2$ with $(Bpin)_2Pz$ in a 1:4 mole ratio is complete within 2 hours at $80^\circ C$ in THF, forming the diamagnetic dinitrosyl iron complex (DNIC) $(DIM)Fe(NO)_2$ in 88% yield (Scheme 3).⁴⁶ The organic byproducts $(Bpin)_2O$ and pyrazine are characterized by 1H NMR spectroscopy in the correct stoichiometric intensities, and these 1H NMR reporters are useful in all deoxygenations for determining the number of oxygens removed with an appropriate internal intensity standard. The

(DIM)Fe(NO)₂ complex is diamagnetic, consistent with other {Fe(NO)₂}¹⁰ complexes. This transformation represents an overall 8-electron reduction of 2 NO₃⁻ to 2 Fe(NO)₂, with the 8 electrons furnished by the four reduced pyrazines. The (DIM)Fe(NO)₂ complex is unreactive towards more (Bpin)₂Pz, which highlights the stability of the {Fe(NO)₂}¹⁰ DNIC.



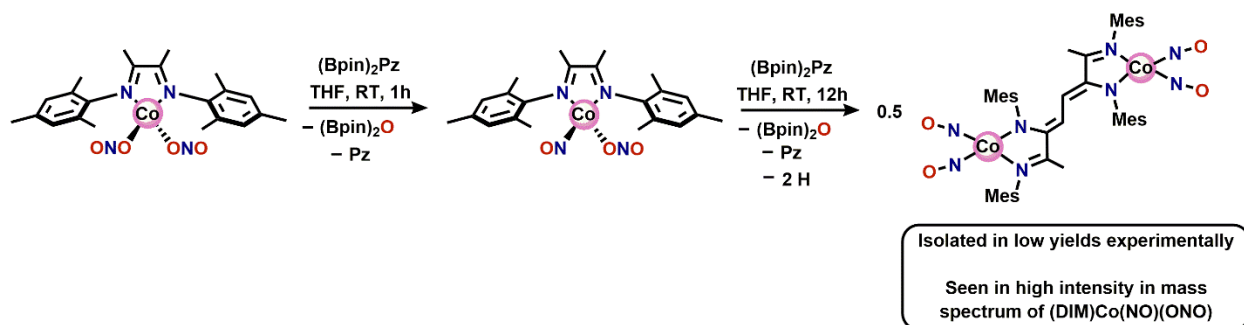
Scheme 3. Quadruple deoxygenation of an iron bis-nitrate complex to yield a dinitrosyl iron complex.

Deoxygenation of Ni(NO_x)₂. With the inability to deoxygenate beyond {Fe(NO)₂}¹⁰, we moved later in the first row transition metal series to nickel, where no Ni(NO)₂ complexes are known. To explore the deoxygenation chemistry of nickel bis-nitrate and bis-nitrite complexes, we synthesized both (DIM)Ni(NO₃)₂ and (DIM)Ni(NO₂)₂.⁴⁸ Seeking stepwise deoxygenation, the reaction of (DIM)Ni(NO₂)₂ with (Bpin)₂Pz in a 1:1 mole ratio results in the formation of the diamagnetic complex (DIM)Ni(NO)(κ¹-ONO) (80 % yield), which is tetrahedral and Ni(0). The mixed nitrito/nitrosyl complex reacts with more (Bpin)₂Pz in a 2:3 ratio to form the dimeric [(DIM)Ni(NO)]₂ complex (75% yield), which is held together purely by a Ni–Ni bond. The reduced nitrogen is proven to be N₂O *via* gas phase and solution infrared spectroscopy, and isotopic labelling experiments indicate that the N–N bond formation occurs within a bimetallic, Ni₂ unit. We speculate that single deoxygenation of (DIM)Ni(NO)(κ¹-ONO) generates a transient di-nitrosyl complex which undergoes intermolecular coupling to liberate N₂O. The [(DIM)Ni(NO)]₂ dimer reacts cleanly with NO gas to accomplish nitric oxide disproportionation and form (DIM)Ni(NO)(ONO) with concomitant N₂O loss. Therefore, a synthetic cycle can be constructed for the disproportionation of nitric oxide using (Bpin)₂Pz as the deoxygenating agent. Attempts to deoxygenate the bis-nitrate or bis-nitrite complexes with elevated temperatures resulted in DIM ligand loss, followed by polymerization as shown in Scheme 4. The polymerization is still accompanied by N₂O loss, and the nickel metal centers in the polymeric structures obtained are bridged by an OBpin⁻ ligand, which is evidence for the ability of the boryl reduced heterocycles to operate *via* concerted, single boryl transfer. The reactivity in Scheme 4 proceeds analogously when (Bpin)₂Pz is replaced by (Bpin)₂Bpy, with the polymeric structure linked through 4,4'-bipyridine instead of pyrazine.



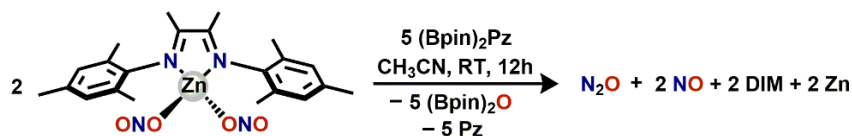
Scheme 4. Summary of reductive deoxygenation of nickel bis-nitrite complex using (Bpin)₂Pz, showing divergent reactivity based on reaction conditions. The stoichiometry for the elevated temperature reaction is 2 (DIM)Ni(NO₂)₂: 4 (Bpin)₂Pz.

Deoxygenation of Co(NO₂)₂. In each of the foregoing, reductive deoxygenation terminates at a known class of M(NO)_x products. In contrast, (L)Co(NO)₂ species are unknown, where L is a neutral, bidentate donor. With the success of deoxygenation of bis-oxyanion compounds using iron and nickel, we first sought single deoxygenation of a cobalt bis-nitrite species, (DIM)Co(NO₂)₂.⁴⁹ The reaction of (DIM)Co(NO₂)₂ with (Bpin)₂Pz in a 1:1 mole ratio proceeds with a color change from brown to purple in the time of mixing at 25 °C, resulting in the formation of (DIM)Co(NO)(ONO) (65% yield), similar to the single deoxygenation of (DIM)Ni(NO₂)₂ (Scheme 5). In contrast to the monodenticity of the nitrito ligand in (DIM)Ni(NO)(ONO), the nitrito is quasi-bidentate for cobalt, a result of the cobalt complex having 17 valence electrons with the nitrito ligand being only κ¹-ONO. The Co–N–O nitrosyl angle is 174.26, indicating NO⁺ and Enemark-Feltham designation {CoNO}⁹. The reaction of (DIM)Co(NO₂)₂ with (Bpin)₂Pz in a 1:2 mole ratio results in a dimeric [(DIM-2H)Co(NO)₂]₂ complex isolated in low yields, a result of two radical (DIM-2H)Co(NO)₂ units coupling through the doubly H-atom abstracted DIM backbone. The H-atom abstraction is attributed to a high energy Co intermediate generated in situ during deoxygenation. Interestingly, [(DIM-2H)Co(NO)₂]₂⁺ is seen with high intensity in the ESI⁺ mass spectrum of (DIM)Co(NO)(ONO), along with [(DIM)Co(NO)₂]⁺. The inability of reductive borylation to form (DIM)Co(NO)₂ is due to the reducing synthetic conditions and redox participation by the allylic DIM methyls in route to the crystallographically characterized product. This result also underscores the propensity of cobalt dinitrosyl complexes to adhere to the {CoNO}¹⁰ electronic structure, while the desired neutral (DIM)Co(NO)₂ complex would have an added electron to adopt a {CoNO}¹¹ electronic structure.



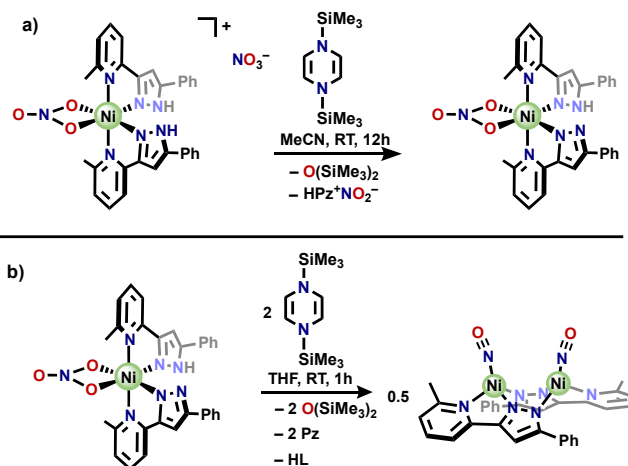
Scheme 5. Summary of reductive deoxygenation of $(\text{DIM})\text{Co}(\text{NO}_2)_2$ using $(\text{Bpin})_2\text{Pz}$.

Deoxygenation of $\text{Zn}(\text{NO}_x)_2$. Due to the inability of zinc to participate in strong π -backbonding, zinc nitrosyls are unknown. With this in mind, we were interested in product selectivity upon deoxygenation of nitrogen oxanions coordinated to zinc. Both $(\text{DIM})\text{Zn}(\text{NO}_2)_2$ and $(\text{DIM})\text{Zn}(\text{NO}_3)_2$ are synthesized in high yields, and the reaction of $(\text{DIM})\text{Zn}(\text{NO}_2)_2$ with $(\text{Bpin})_2\text{Pz}$ in a 1:2.5 mole ratio in THF results in complete consumption of $(\text{DIM})\text{Zn}(\text{NO}_2)_2$ and $(\text{Bpin})_2\text{Pz}$ after 12 hours, as well as the formation of equimolar $(\text{Bpin})_2\text{O}$ and pyrazine (Scheme 6).⁴⁹ The diamagnetic product formed is confirmed to be free DIM ligand by ^1H NMR, and a grey precipitate is confirmed to be metallic zinc by X-ray photoelectron spectroscopy (XPS). Analysis of the headspace after reactivity by gas phase IR shows the presence of both N_2O and NO , and the overall balanced reaction produces 2 moles of NO for each mole of N_2O . The same reactivity is observed between $(\text{DIM})\text{Zn}(\text{NO}_3)_2$ and $(\text{Bpin})_2\text{Pz}$ in a 1:3.5 mole ratio, although it requires elevated temperatures. The need for heating in the bis-nitrate case illustrates the kinetic inertness of nitrate, despite being in a higher oxidation state than nitrite.



Scheme 6. Deoxygenation of $(\text{DIM})\text{Zn}(\text{NO}_2)_2$ using $(\text{Bpin})_2\text{Pz}$.

Deoxygenation of $(\text{HL})(\text{L}^-)\text{Ni}(\text{NO}_3)$. With several results involving metal complexes with multiple N-oxanions coordinated, we sought deoxygenation of a mono-nitrate complex. To this end, we synthesized $[(\text{HL})_2\text{Ni}(\text{NO}_3)]\text{NO}_3$ ($\text{HL} = 2\text{-methyl-6-[5(3)\text{-phenyl-1H-pyrazol-3(5)-yl}]}$) which reacts with $(\text{SiMe}_3)_2\text{Pz}$ in a 1:1 mole ratio to form $(\text{HL})(\text{L}^-)\text{Ni}(\text{NO}_3)$ with loss of $(\text{SiMe}_3)_2\text{O}$ and the pyrazine salt $\text{HPz}^+\text{NO}_2^-$ (Scheme 7).⁵⁰ This reaction represents a unique example where the re-aromatized pyrazine, following silyl transfer, acts as a base and deprotonates the acidic N–H proton of HL, departing with the deoxygenated NO_2^- . The resulting Ni(II) mononitrate complex reacts with $(\text{SiMe}_3)_2\text{Pz}$ in a 1:2 mole ratio to form the dimeric nickel nitrosyl complex $[(\text{L}^-)\text{Ni}(\text{NO})]_2$, which is bridged through the deprotonated pyrazole. This result indicates that $(\text{SiMe}_3)_2\text{Pz}$ is sufficient to deoxygenate a mononitrate to a nitrosyl ligand and shows that deprotonation of acidic protons on a ligand *via* the emerging pyrazine base can be used for the assembly of bimetallic pyrazolate complexes.



Scheme 7. a) synthesis of $(HL)(L^-)Ni(NO_3)$ and b) deoxygenation of $(HL)(L^-)Ni(NO_3)$ to yield the dimeric $[(L^-)Ni(NO)]_2$.

Metal influence on nitrogen product selectivity. Importantly, with the exception of $AgNO_x$, coordination to a transition metal is required for reductive silylation/borylation of the nitrogen oxyanions. The reduced heterocycles are unreactive towards $NaNO_x$ or $(PPN)NO_x$ ($PPN =$ bis(triphenylphosphine)iminium) but react with $AgNO_x$ in the time of mixing to generate Ag metal, the corresponding boryl or silyl ether, and NO gas. A transition metal is necessary for the formation of value-added products beyond nitric oxide, including products containing new N-N bonds. With a suite of deoxygenations using different ancillary ligands and different metals, we begin to see trends in product selectivity of reduced nitrogen containing byproducts. For earlier to mid 3d transition metals, such as chromium and iron, the reduced nitrogen oxyanion is retained by the metal center as either nitrosyl or di-nitrosyl respectively. As we move towards transition metals with increased d-electron counts, we begin to disfavor the coordination of reduced nitrogen and instead favor the liberation of N_xO gases ($X = 1$ or 2). In particular, with the bis-oxyanion DIM compounds, iron retains two nitrosyls, nickel retains one nitrosyl with N_2O liberation, and zinc retains no reduced nitrogen coordinated to the metal center with stoichiometric N_2O and NO liberation. Interestingly, for the deoxygenation of $(DIM)Zn(NO_2)_2$, the balanced reaction closely mirrors that of the stepwise deoxygenation of $(DIM)Ni(NO_2)_2$; however, a $[(DIM)Zn(NO)]_2$ dimer is not thermodynamically stable and instead we observe the constituent parts of the M-M dimer: free DIM, free NO gas, and zinc metal. This is consistent with the trend of increased d-electron count disfavoring coordinated reduced nitrogen and instead leading to gaseous reduced nitrogen products (Figure 4).

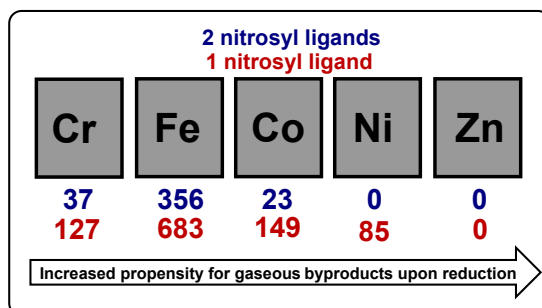


Figure 4. Number of mononitrosyl and dinitrosyl complexes in the CCSD complexes of 1st row transition metals used for nitrogen oxyanion reduction in our group. For the mononitrosyl numbers, the dinitrosyl complexes have been subtracted out.

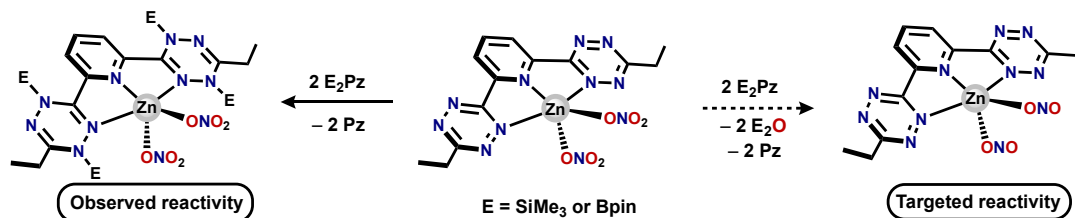
Number of NO_x^- coordinated influence on product selectivity. We report with both the $(DIM)Ni$ and $(DIM)Zn$ complexes that the incorporation of two nitrogen oxyanions on one metal center creates a unique opportunity for N–N bond formation and liberation of N_2O . Deoxygenation of the mono-nitrate complex $(HL)(L^-)Ni(NO_3)$ leads to the formation of dimeric $[(L^-)Ni(NO)]_2$, where one nitrate per nickel is reduced to nitrosyl. The deoxygenation of $(HL)(L^-)Ni(NO_3)$ is closely related to the deoxygenation of $(DIM)Ni(NO_2)_2$ to form $[(DIM)Ni(NO)]_2$; however, the incorporation of a second nitrogen oxyanion in $(DIM)Ni(NO_2)_2$ compared to $(HL)(L^-)Ni(NO_3)$ leads to N–N bond formation and N_2O liberation. Thus far, we have not observed any N–N coupled byproducts via deoxygenation of mono-nitrogen oxyanion complexes.

Mechanism of formal B- or Si-radical transfer from reduced heterocycles. For several of the metal-free reductions of organonitrogen compounds, we observed a strong solvent effect on the reduction. Notably, with reductive silylation of substituted pyrazines, we found the reaction

proceeded much more quickly in acetonitrile than in benzene.⁴⁵ The reactivity shown with AgNO_x (*vide supra*) indicates that a nitrate or nitrite salt with a reducible cation is susceptible to reactivity with the electron rich heterocycles. Both observations support a mechanism of outer sphere electron transfer (OSET) from the electron rich reduced N-heterocycles. Direct evidence for OSET from $(\text{Bpin})_2\text{Bpy}$ was observed in the deoxygenation of $(\text{DIM})\text{Ni}(\text{NO})(\text{ONO})$ with $(\text{Bpin})_2\text{Bpy}$. Mixing these two reagents together in a 1:1 mole ratio results in an immediate color change from brown to dark green, and the monoanionic radical $[(\text{DIM})\text{Ni}(\text{NO})(\text{ONO})]^-$ was observed by IR and EPR spectroscopy. The same monoanion $[(\text{DIM})\text{Ni}(\text{NO})(\text{ONO})]^-$ was synthesized from $(\text{DIM})\text{Ni}(\text{NO})(\text{ONO})$ and $(\text{Cp}^*)_2\text{Co}$ to confirm the outer sphere electron transfer.

Despite our direct evidence for OSET from $(\text{Bpin})_2\text{Bpy}$, there are still many mechanistic questions pertaining to nitrogen oxyanion reduction. Do these reduced N-heterocycles always engage in OSET as the first mechanistic step, or is there a second mechanistic pathway that involves concerted transfer of silyl or boryl radical? Are the silyl vs. boryl reduced heterocycles mechanistically distinct, or will the mechanism of reduction be independent of the E substituent? These questions are currently being asked and researched with “H” transfer, where the mechanism can be proton-coupled electron transfer (PCET), concerted hydrogen atom transfer, and synchronous vs. asynchronous PCET.⁵¹⁻⁵⁶ There are many mechanistic complexities and subtleties with “H” transfer, and we hypothesize that these nuances are also present with “E” transfer from the reduced heterocycles. For $[(\text{DIM})\text{Ni}(\text{NO})(\text{ONO})]^-$, the electron resides in the DIM ligand π^* orbitals; therefore, the redox-active DIM ligand may encourage OSET. New mechanistic insight may be gained by replacing redox-active DIM with a bidentate phosphine ligand that cannot accept an electron. Importantly, the ability of these reduced N-heterocycles to participate in OSET contrasts with B_2pin_2 or $(\text{SiMe}_3)_2$ and represents a benefit of the N-heterocyclic shuttles over using the unpolarized Si–Si or B–B reagents.

Experimental Challenges. Each nitrate or nitrite complex we have synthesized has been reactive towards these reduced N-heterocycles, with some requiring mild heating. However, there are experimental challenges that accompany the reductive silylation and borylation we have executed. We work with a variety of redox-active ligands and most are unreactive and not “damaged” by reactivity with the reduced N-heterocycles. However, with the bis-tetrazinyl-pyridine (btzp) ligand, we observed silylation/borylation of the tetrazine arms instead of reactivity with NO_x^- ligands (Scheme 8).⁵⁷ Reducible moieties on ancillary ligands (e.g. imines) can compete with oxyanion ligands for reduction by the N-heterocycles employed for deoxygenation.



Scheme 8. Example of a redox-active ligand preferentially reacting with the reduced N-heterocycles over the nitrogen oxyanion ligands.

Another experimental challenge is coordination of the re-aromatized heterocycles, whether that be pyrazine or 4,4'-bipyridine. The heterocycles are weak σ -bases and having several equivalents in solution after deoxygenation can encourage coordination and even polymerization, as the N-heterocycles can bridge two metal centers. Particularly, with $(\text{DIM})\text{Ni}(\text{NO}_2)_2$ and $(\text{DIM})\text{Ni}(\text{NO}_3)_3$

deoxygenation at elevated temperatures leads to DIM loss and yields pyrazine or 4,4'-bipyridine polymers with the repeat unit $\text{Ni}_2(\text{NO})_2(\text{OBpin})_2(\text{Pz})$ or $\text{Ni}_2(\text{NO})_2(\text{OBpin})_2(\text{Bpy})$ (Scheme 4). If needed, increasing steric bulk on the reduced heterocycles, such as tetramethyl pyrazine or 2,6-dimethyl-4,4'-bipyridine, can inhibit polymerization or metal coordination of the E shuttle.

The other byproducts of reduction, either $(\text{SiMe}_3)_2\text{O}$ or $(\text{Bpin})_2\text{O}$, are benign and unreactive towards the metal products, and $(\text{SiMe}_3)_2\text{O}$ is volatile and easily removed in vacuo. Re-crystallization of the metal complex synthesized is usually sufficient to remove $(\text{Bpin})_2\text{O}$.

Future Directions and Outlook

While most reported results involve metal complexes with multiple oxanion ligands, we hypothesize an attractive future direction focuses on mono- NO_x^- complexes capable of complete deoxygenation to metal nitrides for subsequent functionalization. We demonstrated the ability of these N-heterocycles to deoxygenate nitrate to nitrosyl, and we anticipate that deoxygenation of a mono-nitrosyl complex to a metal nitride is attainable with the potent deoxygenating agents. The synthesis of a metal nitride from deoxygenation is rare, with several examples reported using low-valent vanadium to remove the oxygen.⁵⁸⁻⁶⁰ Our DFT calculations show that deoxygenation of $\text{Cr}(\text{NO})(\text{N}(\text{SiMe}_3)_2)_3$ to the known $\text{Cr}(\text{N})(\text{N}(\text{SiMe}_3)_2)_3$, as well as deoxygenation of proposed $(\text{PNNH})\text{Mn}(\text{CO})(\text{NO})$ to the proposed nitride $(\text{PNNH})\text{Mn}(\text{N})(\text{CO})$ are both quite exergonic.^{46, 61} Metal nitrides display a wide variety of reactivity depending on the electronic character of the metal nitride fragment,⁶² and developing new synthetic methodologies to access metal nitrides from deoxygenation of nitrate and nitrite ligands could lead to transient late metal nitrides that can undergo subsequent functionalization to create new N–C bonds (Figure 5).^{63, 64}

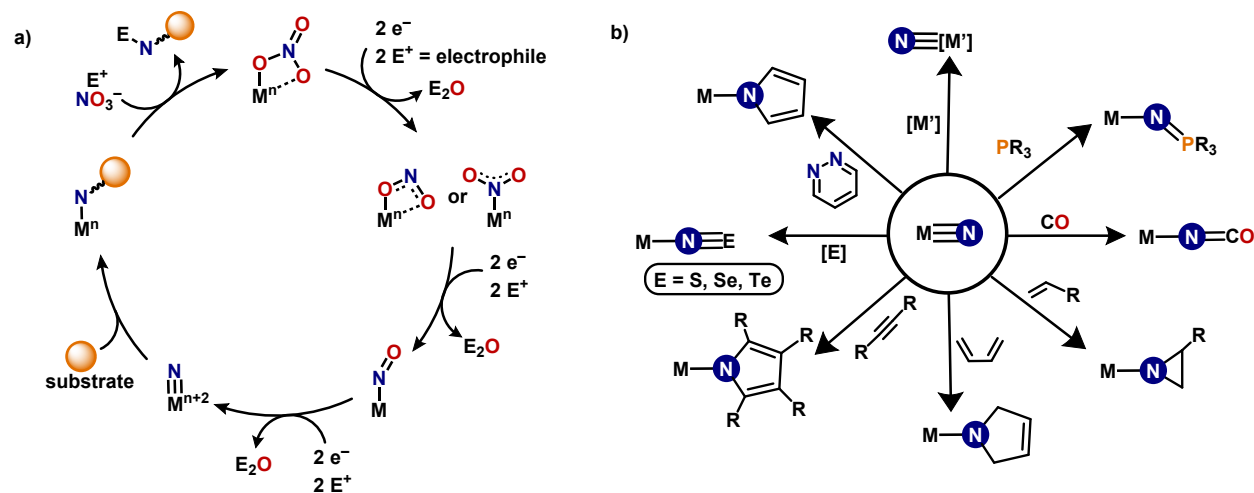
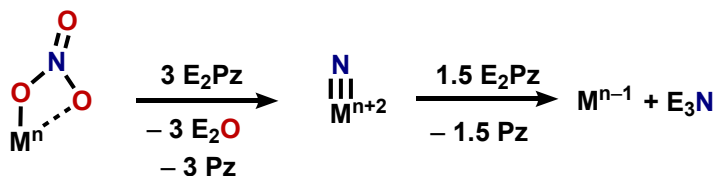


Figure 5. a) Proposed catalytic cycle for the deoxygenation of a metal nitrate to a reactive metal nitride that can be subsequently functionalized and b) proposed substrates used to intercept the nitride derived from nitrate.

In fact, we have preliminary evidence that a transient nickel nitride is synthesized from a nickel nitrate precursor and $(\text{SiMe}_3)_2\text{Pz}$. The choice of metal and ancillary ligands are important when developing synthetic methodology for the synthesis of either isolable or transient, reactive metal nitrides, and some metal nitrides react further with SiMe_3Cl and KC_8 to liberate $(\text{SiMe}_3)_3\text{N}$,⁶⁵ a silylated analogue of NH_3 . Furthermore, the Mezailles group recently reported the catalytic reduction of N_2 to borylamine using a molybdenum pincer complex.^{66, 67} With this in mind, we

anticipate that $(\text{SiMe}_3)_3\text{N}$ or $(\text{Bpin})_3\text{N}$ could be synthesized from nitrate via stepwise deoxygenation and subsequent silylation or borylation of the nitride (Scheme 9).



Scheme 9. Proposed formation of either $(\text{SiMe}_3)_3\text{N}$ or $(\text{Bpin})_3\text{N}$ from a metal nitrate starting material.

Although some nitrides are synthesized from bond cleavage of molecular N_2 ,⁶⁸ many rely on either thermal- or photo-induced N_2 loss from an azide precursor.^{69, 70} Accessing molecular nitrides from nitrate instead of azides not only alleviates the need to work with potentially explosive reagents, but also incorporates reduction of the ubiquitous environmental pollutant.

We used several variants of reduced heterocycles thus far, including $(\text{SiMe}_3)_2\text{Pz}$, $(\text{Bpin})_2\text{Pz}$, $(\text{Me}_4\text{SiMe}_3)_2\text{Pz}$, and $(\text{Bpin})_2\text{Bpy}$. For metal-mediated deoxygenations, the silylated and borylated heterocycles furnish identical reactivity; however, thermodynamic calculations with the silylated pyrazine are consistently more exergonic.⁴⁶ While these reagents have proven quite successful, other reduced heterocycles should be explored for deoxygenation. Sugimoto showed that the most efficient catalyst for diboration of functionalized pyrazines was 2,6-dichloro-4,4'-bipyridine, citing the inductive effect of the chlorine substituents on the bipyridine.⁴⁴ Furthermore, although we have not employed the $(\text{SiMe}_3)_2\text{Bpy}$ reductant, Mashima showed that it is more reducing than $(\text{SiMe}_3)_2\text{Pz}$ and $(\text{Me}_4\text{SiMe}_3)_2$.⁴⁰ Some single nitrogen heterocycles that are used for a variety of organic transformations, including pinacol coupling, are strategically substituted pyridines.⁷¹⁻⁷⁴ The single nitrogen heterocycles are generally para-substituted pyridines with an electron withdrawing group, such as CN or CO_2Me , and react with B_2pin_2 to form mono-borylated pyridine-based radicals that deliver a single Bpin substituent. The mono-borylated substituted pyridines may operate via a mechanistic pathway distinct from the di-borylated N-heterocycles, providing an opportunity for study of single borylation of nitrogen oxyanion ligands. Even in the absence of mechanistic clarity, pyridine as a Bpin shuttle provides both steric and electronic tunability that can be useful in expanding synthetic methodology for oxyanion deoxygenation.

All the deoxygenations we reported were done stoichiometrically; however, with reductive borylation, there is an opportunity to make nitrogen oxyanion reduction catalytic with respect to the B_2pin_2 shuttle, whether that be pyrazine, bipyridine, or pyridine. The overall reduction of nitrate to nitride or NH_3 (both nitrogen atoms at the lowest possible oxidation state) is a demanding process, including 8 electrons and 9 protons in the case of ammonia. Homogenous systems that facilitate nitrate reduction often require harsh reaction conditions; therefore, the development of a catalytic system that uses mild conditions and commodity chemicals from nitrate reduction is a noble pursuit.

We have focused our research efforts exclusively on nitrogen oxyanion reduction; however, we anticipate that the principles learned from N-oxyanion reduction could be extended to other, more challenging oxyanions, including perchlorate, phosphate, and carbonate. There is precedence for perchlorate reduction using a bioinspired iron complex that also performs nitrate reduction.^{32, 75} An inherent challenge with perchlorate and phosphate reduction is coordinating these weak nucleophiles to transition metal centers. While many transition metal perchlorate and carbonate complexes are crystallographically characterized, phosphate complexes are much rarer.

Recently, Schneider reported the synthesis of a rhenium metaphosphite complex via double oxygen atom transfer to a rhenium phosphide.⁷⁶ The deoxygenation of these more difficult oxyanions would require careful design of a metal complex that could stabilize high energy intermediates, and potentially have secondary coordination sphere effects that would encourage binding of the poor nucleophiles.

Conclusion

We showed that silyl- and boryl- N-heterocycles are reactive towards nitrogen oxyanions coordinated to transition metal electrophiles and are promising candidates for the downstream synthesis of value-added products from nitrate/nitrite reduction. While we have many experimental and computational results, we emphasize that there is still much to be explored including a focus on mono-nitrate complexes, altering the metal and ancillary ligands from those shown here, exploring new N-heterocycles for SiMe₃ and Bpin transfer, and studying other oxyanions. The synthetic methodology for deoxygenation of N-oxyanions can be applied to a broad range of systems, and in general finding new approaches for silylation or borylation should benefit a wide array of chemical transformations. If the deoxygenation approach delivers a new synthetic route to nitride complexes, then the current efforts to broaden bond formation to nitrides will have broader significance than simply nitrides from N₂.

Conflicts of interest

There are no conflicts of interest to declare.

Acknowledgements

The summarized work was supported by the Indiana University Office of Vice President for research and the National Science Foundation, Chemical Synthesis Program (SYN), by Grant CHE-1955887 and Grant CHE-1362127.

We thank Kenneth G. Caulton for his support and guidance throughout the projects summarized in this manuscript.

1. V. Smil, *MIT Press*, 2001.
2. W. K. Dodds, W. W. Bouska, J. L. Eitzmann, T. J. Pilger, K. L. Pitts, A. J. Riley, J. T. Schloesser and D. J. Thornbrugh, *Environ. Sci. Technol.*, 2009, **43**, 12-19.
3. M. Könneke, A. E. Bernhard, J. R. de la Torre, C. B. Walker, J. B. Waterbury and D. A. Stahl, *Nature*, 2005, **437**, 543-546.
4. R. J. Diaz and R. Rosenberg, *Science*, 2008, **321**, 926.
5. D.-P. Häder, A. T. Banaszak, V. E. Villafañe, M. A. Narvarte, R. A. González and E. W. Helbling, *Sci. Total Environ.*, 2020, **713**, 136586.
6. J. G. Morris, *Annu. Rev. Energy Env.*, 1999, **24**, 367-390.
7. R. J. Park, D. J. Jacob, B. D. Field, R. M. Yantosca and M. Chin, *J. Geophys. Res. Atmos.*, 2004, **109**.
8. D. P. Butcher and A. A. Gewirth, *Nano Energy*, 2016, **29**, 457-465.
9. S. Hamid, S. Bae and W. Lee, *Chem. Eng. J.*, 2018, **348**, 877-887.
10. S. Jung, S. Bae and W. Lee, *Environ. Sci. Technol*, 2014, **48**, 9651-9658.
11. C. Su and R. W. Puls, *Environ. Sci. Technol*, 2004, **38**, 2715-2720.
12. I. Zhu and T. Getting, *Environ. Technol. Rev.*, 2012, **1**, 46-58.

13. S. Guo, K. Heck, S. Kasiraju, H. Qian, Z. Zhao, L. C. Grabow, J. T. Miller and M. S. Wong, *ACS Catal.*, 2018, **8**, 503-515.
14. N. Zhu, Y. Wu, J. Tang, P. Duan, L. Yao, E. R. Rene, P. K. Wong, T. An and D. D. Dionysiou, *Environ. Sci. Technol.*, 2018, **52**, 8617-8626.
15. S. Challagulla, K. Tarafder, R. Ganesan and S. Roy, *J. Phys. Chem. C*, 2017, **121**, 27406-27416.
16. Z. Geng, Z. Chen, Z. Li, X. Qi, X. Yang, W. Fan, Y. Guo, L. Zhang and M. Huo, *Dalton Trans.*, 2018, **47**, 11104-11112.
17. N. Krasae and K. Wantala, *Appl. Surf. Sci.*, 2016, **380**, 309-317.
18. S. Tawkaew, Y. Fujishiro, S. Yin and T. Sato, *Colloids Surf. A Physicochem. Eng. Asp.*, 2001, **179**, 139-144.
19. V. Rosca, M. Duca, M. T. de Groot and M. T. M. Koper, *Chem. Rev.*, 2009, **109**, 2209-2244.
20. J. Shen, Y. Y. Birdja and M. T. M. Koper, *Langmuir*, 2015, **31**, 8495-8501.
21. W. Teng, N. Bai, Y. Liu, Y. Liu, J. Fan and W.-x. Zhang, *Environ. Sci. Technol.*, 2018, **52**, 230-236.
22. S. Xu, D. C. Ashley, H.-Y. Kwon, G. R. Ware, C.-H. Chen, Y. Losovyj, X. Gao, E. Jakubikova and Jeremy M. Smith, *Chem. Sci.*, 2018, **9**, 4950-4958.
23. S. E. Braley, J. Xie, Y. Losovyj and J. M. Smith, *J. Am. Chem. Soc.*, 2021, **143**, 7203-7208.
24. W. R. Marks, D. F. Baumgardner, E. W. Reinheimer and J. D. Gilbertson, *Chem. Commun.*, 2020, **56**, 11441-11444.
25. M. K. Assefa, G. Wu and T. W. Hayton, *Chem. Sci.*, 2017, **8**, 7873-7878.
26. C. Uyeda and J. C. Peters, *J. Am. Chem. Soc.*, 2013, **135**, 12023-12031.
27. L. T. Elrod and E. Kim, *Inorg. Chem.*, 2018, **57**, 2594-2602.
28. J. Gwak, S. Ahn, M.-H. Baik and Y. Lee, *Chem. Sci.*, 2019, **10**, 4767-4774.
29. J.-X. Liu, D. Richards, N. Singh and B. R. Goldsmith, *ACS Catal.*, 2019, **9**, 7052-7064.
30. P. H. van Langevelde, I. Katsounaros and M. T. M. Koper, *Joule*, 2021, **5**, 290-294.
31. M. Delgado and J. D. Gilbertson, *Chem. Commun.*, 2017, **53**, 11249-11252.
32. C. L. Ford, Y. J. Park, E. M. Matson, Z. Gordon and A. R. Fout, *Science*, 2016, **354**, 741-743.
33. W. Kaim, *J. Am. Chem. Soc.*, 1983, **105**, 707-713.
34. W. Kaim, *J. Chem. Soc., Perkin Trans. 2*, 1985, DOI: 10.1039/P29850001633, 1633-1637.
35. T. Saito, H. Nishiyama, H. Tanahashi, K. Kawakita, H. Tsurugi and K. Mashima, *J. Am. Chem. Soc.*, 2014, **136**, 5161-5170.
36. H. Nishiyama, H. Hosoya, B. F. Parker, J. Arnold, H. Tsurugi and K. Mashima, *Chem. Commun.*, 2019, **55**, 7247-7250.
37. H. Tsurugi, H. Tanahashi, H. Nishiyama, W. Fegler, T. Saito, A. Sauer, J. Okuda and K. Mashima, *J. Am. Chem. Soc.*, 2013, **135**, 5986-5989.
38. H. Tsurugi and K. Mashima, *Acc. Chem. Res.*, 2019, **52**, 769-779.
39. H. Ikeda, K. Nishi, H. Tsurugi and K. Mashima, *Chem. Sci.*, 2020, **11**, 3604-3609.
40. A. Bhattacharjee, H. Hosoya, H. Ikeda, K. Nishi, H. Tsurugi and K. Mashima, *Chem. Eur. J.*, 2018, **24**, 11278-11282.
41. K. Oshima, T. Ohmura and M. Suginome, *Chem. Commun.*, 2012, **48**, 8571-8573.
42. H. Hosoya, L. C. Misal Castro, I. Sultan, Y. Nakajima, T. Ohmura, K. Sato, H. Tsurugi, M. Suginome and K. Mashima, *Org. Lett.*, 2019, **21**, 24, 9812-9817.
43. T. Ohmura, Y. Morimasa and M. Suginome, *Chem. Lett.*, 2017, **46**, 1793-1796.
44. T. Ohmura, Y. Morimasa and M. Suginome, *J. Am. Chem. Soc.*, 2015, **137**, 2852-2855.
45. D. M. Beagan, I. J. Huerfano, A. V. Polezhaev and K. G. Caulton, *Chem. Eur. J.*, 2019, **25**, 8105-8111.
46. D. M. Beagan, V. Carta and K. G. Caulton, *Dalton Trans.*, 2020, **49**, 1681-1687.
47. J. Seo, A. C. Cabelof, C.-H. Chen and K. G. Caulton, *Chem. Sci.*, 2019, **10**, 475-479.

48. D. M. Beagan, A. C. Cabelof, M. Pink, V. Carta, X. Gao and K. G. Caulton, *Chem. Sci.*, 2021, **12**, 10664-10672.
49. D. M. Beagan, A. C. Cabelof, M. Pink, V. Carta, R. Pepin and K. G. Caulton, *Inorg. Chem.*, 2021, **60**, 22, 17241-17248.
50. A. C. Cabelof, V. Carta and K. G. Caulton, *Chem. Commun.*, 2021, **57**, 2780-2783.
51. D. R. Weinberg, C. J. Gagliardi, J. F. Hull, C. F. Murphy, C. A. Kent, B. C. Westlake, A. Paul, D. H. Ess, D. G. McCafferty and T. J. Meyer, *Chem. Rev.*, 2012, **112**, 4016-4093.
52. R. Tyburski, T. Liu, S. D. Glover and L. Hammarström, *J. Am. Chem. Soc.*, 2021, **143**, 560-576.
53. S. Hammes-Schiffer, *Energy Environ. Sci.*, 2012, **5**, 7696-7703.
54. W. D. Morris and J. M. Mayer, *J. Am. Chem. Soc.*, 2017, **139**, 10312-10319.
55. D. Bím, M. Maldonado-Domínguez, L. Rulišek and M. Srnec, *Proc. Natl. Acad. Sci.*, 2018, **115**, E10287-E10294.
56. M. K. Goetz and J. S. Anderson, *J. Am. Chem. Soc.*, 2019, **141**, 4051-4062.
57. D. M. Beagan, N. A. Maciulis, M. Pink, V. Carta, I. J. Huerfano, C.-H. Chen and K. G. Caulton, *Chem. Eur. J.*, 2021, **27**, 11676-11681.
58. A. S. Veige, L. M. Slaughter, E. B. Lobkovsky, P. T. Wolczanski, N. Matsunaga, S. A. Decker and T. R. Cundari, *Inorg. Chem.*, 2003, **42**, 6204-6224.
59. A. L. Odom, C. C. Cummins and J. D. Protasiewicz, *J. Am. Chem. Soc.*, 1995, **117**, 6613-6614.
60. A. S. Veige, L. M. Slaughter, P. T. Wolczanski, N. Matsunaga, S. A. Decker and T. R. Cundari, *J. Am. Chem. Soc.*, 2001, **123**, 6419-6420.
61. A. C. Cabelof, A. M. Erny, D. M. Beagan and K. G. Caulton, *Polyhedron*, 2021, **200**, 115119.
62. J. M. Smith, in *Progress in Inorganic Chemistry Volume 58*, 2014, DOI: <https://doi.org/10.1002/9781118792797.ch06>, pp. 417-470.
63. I. Klopsch, E. Y. Yuzik-Klimova and S. Schneider, in *Nitrogen Fixation*, ed. Y. Nishibayashi, Springer International Publishing, Cham, 2017, DOI: 10.1007/3418_2016_12, pp. 71-112.
64. B. Schluschaß, J.-H. Bortner, S. Rupp, S. Demeshko, C. Herwig, C. Limberg, N. A. Maciulis, J. Schneider, C. Würtele, V. Krewald, D. Schwarzer and S. Schneider, *JACS Au*, 2021, **1**, 879-894.
65. Y. Tanabe and Y. Nishibayashi, *Coord. Chem. Rev.*, 2019, **389**, 73-93.
66. M. F. Espada, S. Bennaamane, Q. Liao, N. Saffon-Merceron, S. Massou, E. Clot, N. Nebra, M. Fustier-Boutignon and N. Mézailles, *Angew. Chem. Int. Ed.*, 2018, **57**, 12865-12868.
67. S. Bennaamane, M. F. Espada, A. Mulas, T. Personeni, N. Saffon-Merceron, M. Fustier-Boutignon, C. Bucher and N. Mézailles, *Angew. Chem. Int. Ed.*, 2021, **60**, 20210-20214.
68. S. J. K. Forrest, B. Schluschaß, E. Y. Yuzik-Klimova and S. Schneider, *Chem. Rev.*, 2021, **121**, 6522-6587.
69. J. Sun, J. Abbenseth, H. Verplancke, M. Diefenbach, B. de Bruin, D. Hunger, C. Würtele, J. van Slageren, M. C. Holthausen and S. Schneider, *Nature Chem.*, 2020, **12**, 1054-1059.
70. D. M. King, F. Tuna, E. J. L. McInnes, J. McMaster, W. Lewis, A. J. Blake and S. T. Liddle, *Nature Chem.*, 2013, **5**, 482-488.
71. G. Wang, J. Cao, L. Gao, W. Chen, W. Huang, X. Cheng and S. Li, *J. Am. Chem. Soc.*, 2017, **139**, 3904-3910.
72. J. Jo, S. Kim, J.-H. Choi and W.-j. Chung, *Chem. Commun.*, 2021, **57**, 1360-1363.
73. L. Gao, G. Wang, H. Chen, J. Cao, X. Su, X. Liu, M. Yang, X. Cheng and S. Li, *Organic Chemistry Frontiers*, 2020, **7**, 2744-2751.
74. J. Cao, G. Wang, L. Gao, X. Cheng and S. Li, *Chem. Sci.*, 2018, **9**, 3664-3671.
75. M. J. Drummond, T. J. Miller, C. L. Ford and A. R. Fout, *ACS Catal.*, 2020, **10**, 3175-3182.
76. J. Abbenseth, F. Wätjen, M. Finger and S. Schneider, *Angew. Chem. Int. Ed.*, 2020, **59**, 23574-23578.

